

Limits on the Abundance of Galactic Planets From Five Years of PLANET Observations

M. D. Albrow^{1,2}, J. An³, J.-P. Beaulieu⁴, J. A. R. Caldwell⁵,
D. L. DePoy³, M. Dominik⁶, B. S. Gaudi³, A. Gould³, J. Greenhill⁷,
K. Hill⁷, S. Kane^{2,7}, R. Martin⁸, J. Menzies⁵, R. M. Naber⁶, J.-W. Pel⁶,
R. W. Pogge³, K. R. Pollard¹, P. D. Sackett⁶, K. C. Sahu²,
P. Vermaak⁵, P. M. Vreeswijk^{6,9}, R. Watson⁷, A. Williams⁸

The PLANET Collaboration

ABSTRACT

We search for signatures of planets in 43 intensively monitored microlensing events that were observed between 1995 and 1999. Planets would be expected to cause a short (~ 1 day) deviation on an otherwise normal smooth, symmetric, single-lens light curve. We find no such anomalies and infer that less than 1/3 of the $\sim 0.3 M_{\odot}$ stars that typically comprise the lens population have Jupiter-mass companions in the range of semi-major axes $1.5 \text{ AU} < a < 4 \text{ AU}$.

Subject headings: gravitational lensing, planetary systems

¹Univ. of Canterbury, Dept. of Physics & Astronomy, Private Bag 4800, Christchurch, New Zealand

²Space Telescope Science Institute, 3700 San Martin Drive, Baltimore, MD. 21218 U.S.A.

³Ohio State University, Department of Astronomy, Columbus, OH 43210, U.S.A.

⁴Institut d'Astrophysique de Paris, INSU CNRS, 98 bis Boulevard Arago, F-75014, Paris, France

⁵South African Astronomical Observatory, P.O. Box 9, Observatory 7935, South Africa

⁶Kapteyn Astronomical Institute, Postbus 800, 9700 AV Groningen, The Netherlands

⁷Univ. of Tasmania, Physics Dept., G.P.O. 252C, Hobart, Tasmania 7001, Australia

⁸Perth Observatory, Walnut Road, Bickley, Perth 6076, Australia

⁹Astronomical Institute "Anton Pannekoek", University of Amsterdam, Kruislaan 403, 1098 SJ Amsterdam, The Netherlands

1. Introduction

Searches for extra-solar planets are being carried out using several methods. More than 30 planets have been discovered by the doppler-shift technique (Marcy, Cochran, & Mayor 2000). While ground-based astrometric searches have not yielded any definitive detections, the launchings of the *Full-Sky Astrometric Mapping Explorer (FAME)*, the *Space Interferometry Mission (SIM)*, and the *Global Astrometric Interferometer for Astrophysics (GAIA)* are expected to radically improve the sensitivity of this technique (Lattanzi et al. 2000). The occultation method has yielded an important null result for planets in 47 Tuc (Brown et al. 2000), and one confirmation (Charbonneau et al. 2000; Henry et al. 2000) that allowed the density of an extra-solar planet to be determined for the first time. However, all of these methods are fundamentally restricted to planets with orbital times shorter than the experiment, and hence to relatively close (and also generally massive) companions.

Microensing provides a method to search for planets (Mao & Paczyński 1991) that does not suffer from this limitation. When two stars are approximately aligned with an observer, the nearer star (the “lens”) splits the light from the more distant star (the “source”) into two images whose positions and brightnesses change as the relative alignment changes. The characteristic angular scale, θ_E (“Einstein ring”), and timescale, t_E , of such a microensing event are

$$\theta_E = \sqrt{\frac{4G}{c^2} \frac{M}{D_{\text{rel}}}}, \quad t_E = \frac{\theta_E}{\mu_{\text{rel}}}, \quad (1)$$

where M is the mass of the lens, $D_{\text{rel}} \equiv \text{AU}/\pi_{\text{rel}}$, π_{rel} is the lens-source relative parallax, and μ_{rel} is the relative proper motion. Note that $D_{\text{rel}}^{-1} = D_L^{-1} - D_S^{-1}$, where D_L and D_S are the lens and source distances. For typical events seen toward the Galactic bulge, $\theta_E \sim 320 \mu\text{as} (M/0.3 M_\odot)^{1/2}$, which is far too small to resolve directly. However, since the images are magnified, the event can be identified photometrically. For typical bulge events, $\mu_{\text{rel}} \sim 25 \text{ km s}^{-1} \text{ kpc}^{-1}$, so $t_E \sim 20$ days, and hence nightly monitoring is sufficient to find most events. Four groups, OGLE, MACHO, EROS, and MOA have carried out such microensing searches and combined have detected over 700 events, most in the direction of the Galactic bulge (Udalski et al. 2000; Alcock et al. 1997; Afonso et al. 2001; Abe et al. 1997). All four teams developed the ability to recognize these events in real time and electronically alert the community soon after the onset of the event.

If the lens has a planet that lies close to one of the lensed images of the source, that image is further perturbed and the magnification changes significantly during a time t_p ,

$$t_p = \frac{\theta_p}{\theta_E} t_E, \quad \theta_p = \sqrt{\frac{m_p}{M}} \theta_E, \quad (2)$$

where m_p is the mass of the planet. Hence a planet betrays itself as a short (~ 1 day) “bump” on an otherwise normal single-lens light curve (Refsdal 1964; Paczyński 1986). Since the characteristic range of the planet’s effect is θ_p , the naive probability of such a planetary anomaly is $\sim \theta_p/\theta_E = (m_p/M)^{1/2}$ or about 3% for $M/m_p \sim 1000$ (as would be the case for the Sun and Jupiter). However, Gould & Loeb (1992) showed that the probability can be much higher for planets lying relatively close to the Einstein ring of the lensing star, primarily because the effective range of the planet’s action is enhanced to $\sim A\theta_p$ along the planet-star axis when the source is magnified by a factor A . Since $A_{\max} \sim u_0^{-1}$ where u_0 is the impact parameter, detection probabilities are higher in low-impact parameter events. Additional effects further enhance the detection probability in very high magnification events with $A_{\max} \gtrsim 10$ (Griest & Safizadeh 1998), although characterization may then be more complicated if multiple planets are present (Gaudi, Naber & Sackett 1998). While planets as small as the Earth can give rise to detectable signals for suitably small sources, the probability for this to happen declines $\propto m_p^{1/2}$. If photometric precision of about 1-2% can be achieved, however, Jupiter-mass planets present a reasonable probability for detection throughout a wide zone centered on the Einstein ring. For typical lens distances ~ 6 kpc, this sensitivity peaks at projected separations $2 \text{ AU} (M/0.3 M_\odot)^{1/2}$. Since t_p is of order or shorter than the sampling time of the microlensing search teams, Gould & Loeb (1992) advocated setting up a globe-straddling network of observatories to do continuous follow-up observations of alerted events.

The PLANET collaboration was formed in 1995 (Albrow et al. 1996) expressly to carry out such observations and demonstrated in that pilot year that the program was feasible (Albrow et al. 1998). PLANET obtained substantial observing time at four southern locations (Tasmania, Western Australia, South Africa, and Chile) during 1995, 1996, and 1997, and nearly dedicated access to telescopes at all four locations in 1998 and 1999. During these five years, we monitored ~ 50 microlensing events sufficiently well to have good to excellent sensitivity to planets. None of these events displayed a clear photometric anomaly consistent with that of a planet orbiting the lens. We quantify this statement by characterizing the statistical

sensitivity of our five-year data set to planets. We then use these results to build mass-separation exclusion diagrams for the typical Galactic stars (i.e., microlenses) that our survey probes. The basic method of analysis is given in Gaudi & Sackett (2000) and has been illustrated by applying it to one event, OGLE 1998-BUL-14 (Albrow et al. 2000b). The details of its application to the present data set will be given by Albrow et al. (2001).

2. PLANET Five-Year Photometric Dataset

Our data were acquired over five years from six telescopes: the Canopus 1m near Hobart, Tasmania, the Perth/Lowell 0.6m at Bickley, Australia, the Elizabeth 1m at the South African Astronomical Observatory (SAAO) at Sutherland, South Africa, the ESO/Dutch 0.9m at La Silla, Chile, the Yale 1m and the CTIO 0.9m at the Cerro Tololo Interamerican Observatory (CTIO) at La Serena, Chile. The Chilean observations were carried out primarily with the ESO/Dutch (1995-7) and Yale (1998-9) telescopes. Data were collected in Cousins I and Johnson V , with strong emphasis on the former because bulge fields are generally significantly reddened and monitoring must proceed during all lunar phases.

Figure 1 shows PLANET photometry of OGLE 1999-BUL-35, which serves to illustrate many of the characteristics of the data. Observations from four observatories permit round-the-clock monitoring. The median sampling time is about 1 hour. Of course, there are gaps in the data due mostly to weather, but these rarely last as long as a day. The photometric precision (judged by the scatter, not the formal DoPhot photometry errors) is of order 1–2% for points near the peak, which contain most of the sensitivity to planets. Errors on the wing points (necessary to characterize the geometry of the event, see § 4) are larger, a few percent. OGLE 1999-BUL-35 is exceptional in that it is the highest magnification ($A_{\max} = 128$) event for which we obtained precise photometry near the peak of its light curve. Furthermore, it is more densely sampled than typical events to take advantage of its higher sensitivity to planets. The sensitivity of a similar event, OGLE 1998-BUL-14, was analyzed by PLANET (Albrow et al. 2000b); our sample contains about 5 other events with similar detection efficiency. The bulk of events have similar median sampling times of 1 to 2 hours, and typical photometric errors of one to a few percent. Details will be given in Albrow et al. (2001).

3. Event Selection

We begin with the complete sample of Galactic bulge events monitored by PLANET during 1995-1999, discarding those with extremely poor quality or poorly-sampled light curves and those known to contain anomalies characteristic of roughly equal-mass binaries or other anomalies (such as parallax) unrelated to binarity. Normal point-source/point-lens (PSPL) microlensing events are described by

$$F(t) = F_s A(t) + F_b, \quad A[u(t)] = \frac{u^2 + 2}{u(u^2 + 4)^{1/2}}, \quad u(t) = \sqrt{u_0^2 + \frac{(t - t_0)^2}{t_E^2}}, \quad (3)$$

where F is the observed flux (corrected for seeing, Albrow et al. 2000b), F_s is the source flux, F_b is the flux from any background light that is not magnified, u_0 is the impact parameter, and t_0 is the time of closest approach. Separate F_s and F_b are required for each observatory and wave band.

Parallax and equal-mass binary light curve anomalies are identified through explicit modeling. We discard such anomalous light curves from our analysis because we do not currently have the ability to systematically search for planetary signatures in the presence of these secondary effects. We note, however, that none of the excluded light curves shows signs of short duration bumps, except MACHO 97-BLG-41 for which the deviation is explained naturally by binary rotation (Albrow et al. 2000a) rather than a planet orbiting a binary (Bennett et al. 1999).

To eliminate events of particularly poor quality for planet detection, we introduce event selection criteria:

- 1) All data must pass certain quality tests: DoPhot (Schechter, Mateo, & Saha 1993) types 11 and 13 accepted
- 2) There must be at least 20 data points from at least one observatory in one band
- 3) Each observatory-band dataset included must contain at least 10 data points
- 4) The error in u_0 from a combined fit must be less than 50%

If u_0 is not well constrained, then the source’s path through the Einstein ring is not well determined, and hence it is difficult to estimate the sensitivity of the event to planets. When available, we use OGLE and MACHO data to help constrain u_0 , but not to search for planets (Albrow et al. 2001).

4. Systematic Search for Planetary Signatures

The method of measuring the sensitivity of an event to the presence of planets, and at the same time searching for planetary signatures if they are present, is thoroughly described in Albrow et al. (2000b). Very briefly, we obtain a PSPL fit using equation (3), and simultaneously renormalize the photometric errors at each observatory so that the total χ_{PSPL}^2 of this fit is equal to the number of degrees of freedom. For each planet-star mass ratio q and each planet-star projected separation $\theta_E d$, as well as each angle α of the source trajectory relative to the binary axis, we find the best fit to the remaining parameters $(t_0, t_E, u_0, F_s, F_b)$. The corresponding χ^2 thus yields $\Delta\chi^2 \equiv \chi^2 - \chi_{\text{PSPL}}^2$, for which we set a threshold value $\Delta\chi_{\text{min}}^2 = 60$. If $\Delta\chi^2 > \Delta\chi_{\text{min}}^2$, then the geometry (d, q, α) is excluded. If $\Delta\chi^2 < -\Delta\chi_{\text{min}}^2$, we tentatively conclude that we have detected a planet. The detection efficiency $\epsilon_i(d, q)$ for planets with this (d, q) in event i is then just the fraction of all angles α (out of 2π) that are excluded. We define a “planetary system” as a binary lens with mass ratio $q < 0.01$.

We set the threshold $\Delta\chi_{\text{min}}^2 = 60$ by first noting the continuous distribution of $\Delta\chi^2 \lesssim 50$ in our data. If a significant fraction of these were due to planets, the distribution would extend to much more extreme values, since a small random change in the impact parameter could easily increase $\Delta\chi^2$ to several hundred. Hence, the great majority of these deviations must be due to small unrecognized systematic errors. We therefore set the threshold high enough to exclude this non-planetary source of systematic noise.

This search procedure identifies only two possible candidates, but these are also representatives of two classes of phenomena that must be excluded from our search: irregular variable sources and global-asymmetry anomalies. MACHO 99-BLG-18 has a ~ 2 day anomaly that is consistent with a planet having $q \sim 0.01$. However, analysis of five years of previous MACHO data shows that the source is an irregular red-giant variable that often generates photometric excursions of similar duration and amplitude. We eliminate this and all irregular variables from the analysis because it is impossible to confidently recognize planetary anomalies in such sources. OGLE 99-BUL-36 displays an overall asymmetry that is consistent with a distortion caused by a $q \sim 0.003$ planet. However, a very special planetary geometry is required to produce a global asymmetry (rather than a bump), whereas such asymmetries are a general feature of parallax which must be present at some level in all microlensing

events (Gould, Miralde-Escudé & Bahcall 1994). We exclude all such long-duration global asymmetries. Thus, there are no viable planet candidates out of a total of 43 events.

Rhie et al. (2000) present evidence for a possible Neptune-mass planet in MACHO 98-BLG-35. Even though our data on this event are of comparable quality and temporal coverage, we see no evidence for a planetary anomaly and thus do not confirm the presence of a planet.

5. Exclusion Diagram for Galactic Planets

From the above analysis of each event i , we obtain an efficiency $\epsilon_i(d, q)$ as a function of planetary geometry (d, q) . Let $f(d, q)$ be the fraction of lenses having a planet at (d, q) . The expected number of detections is then $N(d, q) = f(d, q) \sum_i \epsilon_i(d, q)$. If a model predicts N and none is observed, it can be rejected with $P = [1 - \exp(-N)]$ confidence. Hence, fractions $f(d, q) \geq 3 / \sum_i \epsilon_i(d, q)$ can be rejected at 95% confidence. In fact, we employ a more rigorous formula, $P = 1 - \prod_i [1 - f(d, q) \epsilon_i(d, q)]$ which reduces to this naive formula in the limit of $f\epsilon \ll 1$.

Based on this analysis, we build an exclusion diagram (Fig. 2) for planet parameters (d, q) . To convert d and q into physical parameters of planet mass m_p and projected physical separation r_p , we must estimate the typical mass M and physical Einstein radius $D_L \theta_E$ for the events in our sample. The majority of detected microlensing events are almost certainly bulge stars lensing other bulge stars (Kiraga & Paczyński 1994). If the lenses were drawn randomly from the bulge mass function as measured by Zoccali et al. (2000), one would expect the typical mass to be $M \sim 0.3 M_\odot$ and hence the typical timescale to be $t_E \sim 20$ days. However, the median timescale for our sample is 40 days. The difference is probably mainly due to a bias in our selection process: the shorter an event, the less likely that it will be alerted early enough that we will be able to effectively monitor the peak. Without good peak coverage, the event will often fail our selection criterion of less than 50% error in u_0 . From equation (1), a bias toward large t_E will cause biases toward higher M , higher π_{rel} , and lower μ_{rel} . Comparing Figures 1a and 1b from Gould (2000), we infer that most of the dispersion in observed timescales is due to μ_{rel} and π_{rel} , so the bias in terms of mass is likely to be modest. Hence, we

adopt $M \sim 0.3 M_\odot$ and $\pi_{\text{rel}} \sim 40 \mu\text{as}$, and thus $\theta_E \sim 320 \mu\text{as}$. With our convention $D_L = 6 \text{ kpc}$, $q = 0.001 \Rightarrow m_p = 0.3 M_{\text{Jup}}$, and $d = 1 \Rightarrow r_p = 2 \text{ AU}$.

In Figure 3 we present the upper limits for the fraction of lenses with planets over two ranges of semi-major axes a centered on the Einstein ring. In particular, less than 1/3 of lenses have Jupiter-mass companions anywhere in the range of $1.5 \text{ AU} < a < 4.0 \text{ AU}$. To convert from projected separation (Fig. 2) to semi-major axis, we integrate over all orientations assuming circular orbits, $M = 0.3 M_\odot$ and $D_L \theta_E = 2 \text{ AU}$. We calculate efficiencies using both the point-source approximation and allowing for finite source size (Gaudi & Sackett 2000) but find that the difference is negligible. These are the first significant limits on planetary companions of M dwarfs. The orbital periods of planets at these radii are 3 to 15 years. Hence, the outer portion of this region would be difficult to probe using radial-velocity, astrometric, or other techniques.

We thank the EROS, MACHO, and OGLE collaboration for providing the original electronic microlensing event alerts that are the sine qua non of this work, and the MACHO and OGLE collaborations for providing their original data for many of the events. We are especially grateful to the observatories that support our science (Canopus, CTIO, ESO, Perth, SAAO, Yale) via the generous allocations of time that make this work possible, and to those who have donated their time to observe for this program. PLANET acknowledges financial support via award GBE 614-21-009 from the organization for *Nederlands Wetenschappelijk Onderzoek* (Dutch Scientific Research), the Marie Curie Fellowship ERBFMBICT972457 from the European Union, a “coup de pouce 1999” award from the *Ministère de l’Éducation nationale, de la Recherche et de la Technologie, Département Terre-Univers-Environnement*, grants AST 97-27520 and AST 95-30619 from the NSF, and NASA grant NAG5-7589.

REFERENCES

- Abe, F. et al. 1997, Variable Stars and the Astrophysical Returns of the Microlensing Surveys, R. Ferlet, J.-P. Maillard, and B. Raban, eds., (Gif-Sur-Yvette: Editions Frontières), p. 75
- Afonso, C. et al. 2001, in preparation
- Albrow, M. et al. 1996, Astrophysical Applications of Gravitational Lensing, IAU 173, eds., C. Kochanek and J. Hewitt (Dordrecht: Kluwer), p. 227.
- Albrow, M. et al. 1998, ApJ, 509, 687
- Albrow, M. et al. 2000a, ApJ, 534, 894
- Albrow, M. et al. 2000b, ApJ, 535, 176
- Albrow, M. et al. 2001, in preparation
- Alcock, C. et al. 1997, ApJ, 479, 119
- Bennett, D.P., et al. 1999, Nature, 402, 57
- Brown, T.M., et al. 2000, BAAS, 196.0203B
- Charbonneau, D., Brown, T.M., Latham, D.W., & Mayor, M. 2000, 529, L45
- Gaudi, B.S., & Sackett P.D. 2000, ApJ, 528, 256
- Gaudi, B.S., Naber, R.M., & Sackett P.D. 1998, ApJ, 502, L33
- Gould, A. 2000, ApJ, 532, 928
- Gould, A. & Loeb, A. 1992, ApJ, 396, 104
- Griest, K., & Safizadeh, N. 1998, ApJ, 500, 37
- Henry, G.W., Marcy, G.W., Butler, R.P., & Vogt, S.S. 2000, ApJ, 529, L41
- Kiraga, M., & Paczyński, B. 1994, ApJ, 430, L101
- Lattanzi, M.G., Spagna, A., Sozzetti, A., Casertano, S. 2000, MNRAS, in press
- Mao, S., & Paczyński, B. 1991, 374 L37
- Marcy, G.W., Cochran, W.D., & Mayor, M. 2000, Protostars and Planets IV, eds. V. Mannings, A.P. Boss, and S.S. Russell (Tucson: University of Arizona), p. 1285
- Paczynski, B. 1986, ApJ, 304, 1
- Refsdal, S., 1964, MNRAS, 128, 295

Rhie, S.H. et al. 2000, ApJ, 533, 378

Schechter, P.L., Mateo, M., & Saha, A. 1993, PASP, 105, 1342

Udalski, A., Zebrun, K., Szymanski, M., Kubiak, M., Pietrzynski, G., Soszynski, I.,
& Wozniak, P. 2000, Acta Astron. 50, 1

Zoccali, M., S., Cassisi, S., Frogel, J.A., Gould, A., Ortolani, S., Renzini, A., Rich,
R.M. 1999, & Stephens, A. 2000, ApJ, 530, 418

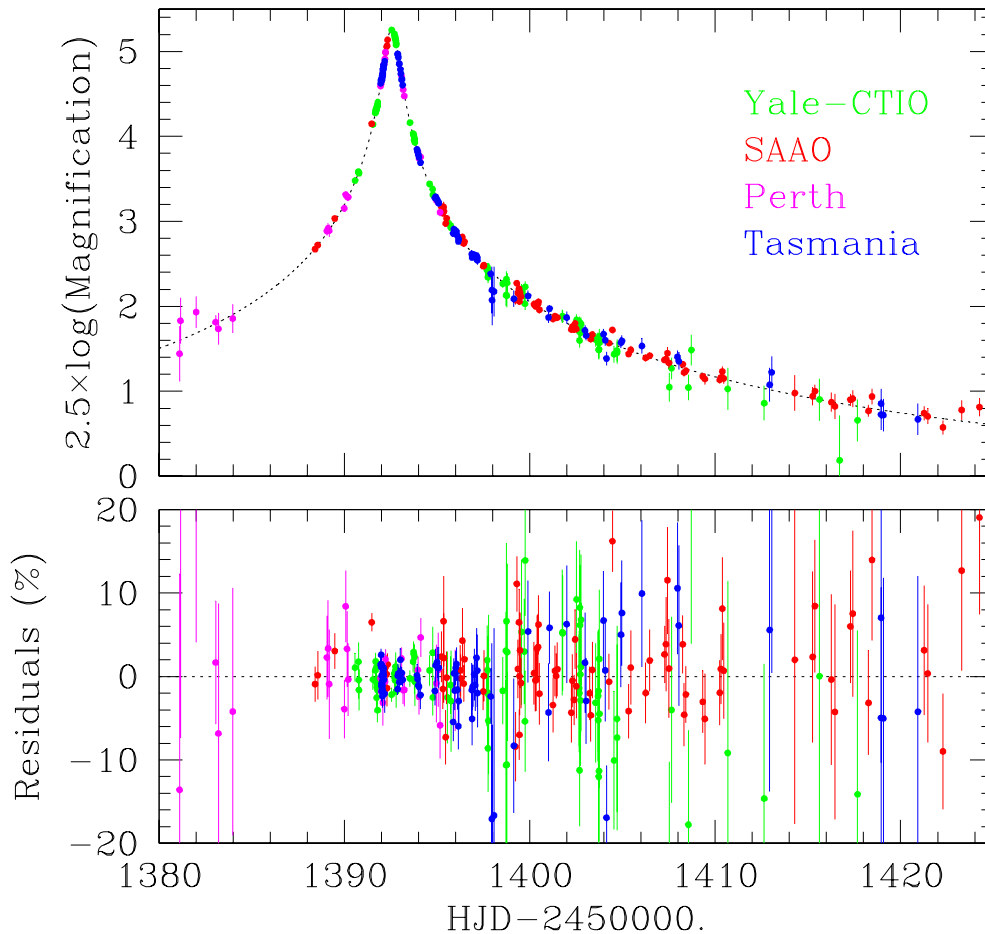


Fig. 1.— PLANET photometry of one microlensing event, OGLE 99-BUL-35, among 43 that were searched for planets. Data from four observatories, Yale-CTIO (green), SAAO (red), Perth (magenta), and Tasmania (blue) permitted round-the-clock coverage except when interrupted by weather. Median sampling is 1 hour. Errors (detailed in the lower, residuals plot) are 1–2% in the peak and a few percent in the wings. These characteristics together with the event’s high magnification imply that it has almost 100% sensitivity to Jupiter-mass planets in the range $0.6 \lesssim d \lesssim 1.6$.

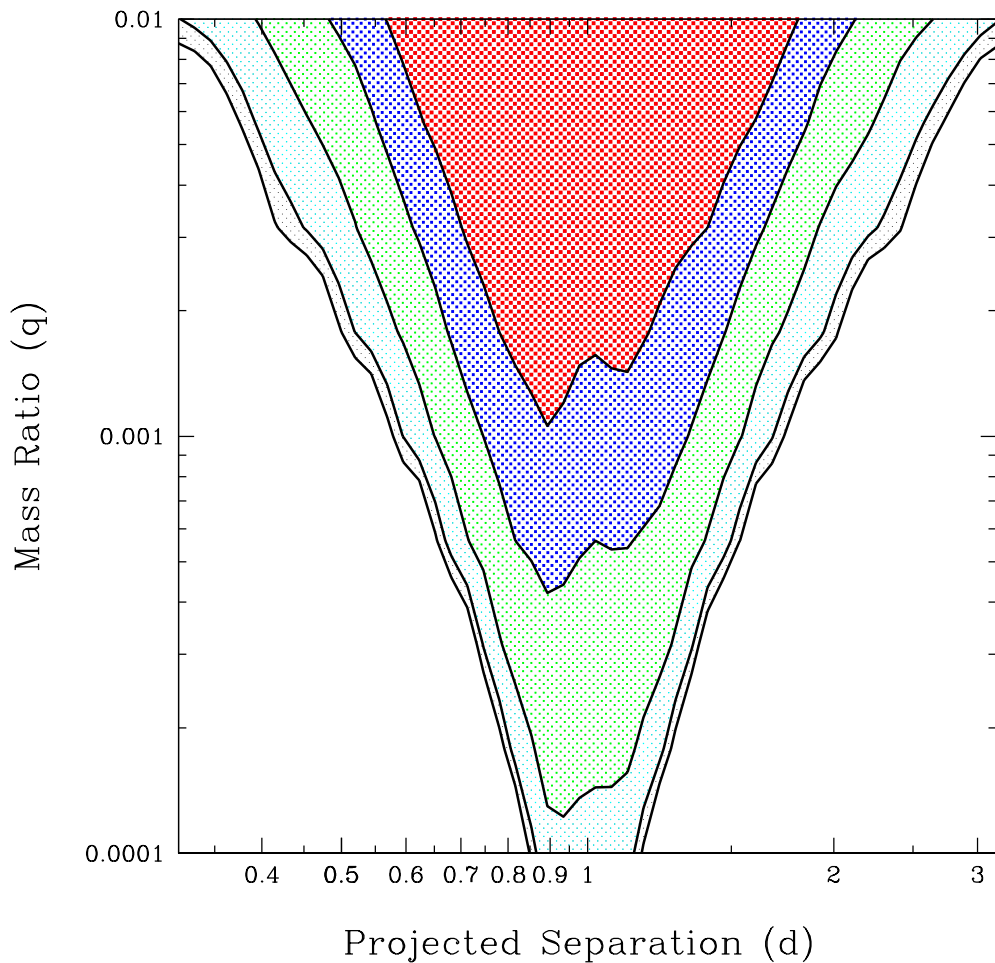


Fig. 2.— Exclusion diagram for pairs of planet parameters (d, q) , where d is the projected separation in units of the Einstein ring, and q is the planet-star mass ratio. The inner contour indicates the (d, q) for which the fraction of lenses with a planet is $f < 1/4$ at 95% confidence. Other contours are for $f < 1/3, 1/2, 2/3,$ and $3/4$. A mass ratio $q = 0.001$ corresponds approximately to $m_p = 0.3 M_{\text{Jup}}$ and a projected separation of $d = 1$ corresponds to a physical projected separation $r_p = 2 \text{ AU}$.

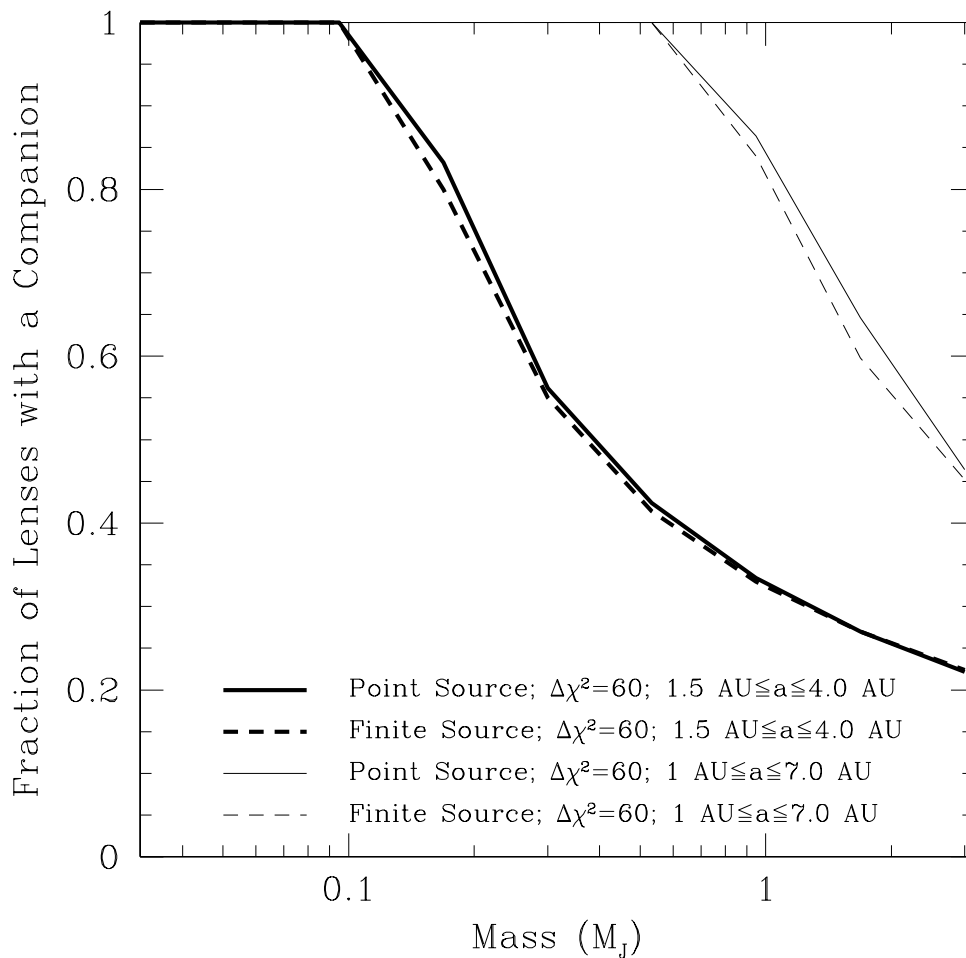


Fig. 3.— Exclusion diagram for planets anywhere in a continuous range of semi-major axes centered on the Einstein ring. Bold curves show the excluded fraction (at 95% confidence) anywhere in the range $1.5 \text{ AU} < a < 4 \text{ AU}$, while solid curves show the fraction for $1 \text{ AU} < a < 7 \text{ AU}$. The dashed curves show the negligible effect of including the finite size of the source in the modeling.